Bioherbicidal Evaluation of *Ammi majus* L.-Derived Silver Nanoparticles in Weed Management

Zhean Luqman Salih[1], Saber Wasman Hamad[1*]

[1]Department of Field Crops and Medicinal Plants, College of Agricultural Engineering Sciences, Salahaddin University- Erbil, Erbi, Kurdistan Region, Iraq
*Corresponding author's email: saber.hamad@su.edu.krd

Abstract

This study explores a green method to create and test silver nanoparticles (AgNPs) using extracts from *Ammi majus* L. leaves for weed control. *Ammi majus* L.is an allelopathic plant, meaning it releases natural compounds (allelochemicals) that can suppress weed growth. However, these compounds break down quickly in the environment, reducing their effectiveness. To solve this, this study has been used in plant-based synthesis to produce AgNPs, which are more stable and efficient. The plant extracts acted as natural reducing and stabilizing agents, avoiding harmful chemicals. UV-Vis spectroscopy confirmed the formation of AgNPs, revealing a peak at 430 nm. Additional tests (FTIR, XRD, SEM, and EDX) were used to analyze the nanoparticles structure and composition. Using varying doses, the synthetic AgNPs' herbicidal efficacy was evaluated on weed seeds. With the highest dose (250 ppm) exhibiting the sharpest suppression of root and shoot development, the results demonstrated a concentration-dependent inhibition of seed germination and seedling growth. These results suggest that *A. majus* -derived AgNPs have strong bioherbicidal qualities and can be used as a sustainable substitute for synthetic herbicides. This technology minimizes the environmental concerns connected with traditional weed management techniques while also reducing the amount of chemicals used in agriculture. In addition to encouraging more research into the long-term ecological consequences and field-level application of plant-based nanoparticles, the study supports their usage in contemporary weed management.

Keywords: Silver nanoparticles (AgNO3), Green synthesis, Bioherbicide, Allelopathy, Weed management.

ISSN 2072-3857

Introduction

Allelopathy signifies biochemical interactions among plants, including microorganisms, through natural compounds, which are termed allelochemicals. These interactions may promote or hinder the survival, growth, and reproduction of adjacent plants [1,31] Allelochemicals enter into the environment through root exudation, leaching, volatilization, or decomposition of plant residues.

[2] perceived allelochemicals as being only harmful; further testing had showed that many of these compounds have two facets to them, acting as an inhibitor when in a high concentration and as a stimulant when in a low concentration for the target organism. This new understanding missed by Rice realigns the evolution of this science back to Molisch's very early definition, with all-important complex ecological roles of [3]. Beginning with the formation of plant communities, allopathy maintains biodiversity and regulates productivity within ecosystems. Though utilized through ancient times in traditional agriculture, this area has too much potential that has been never tapped into by modern agriculture. Allelopathy can sometimes be confused with competition: in allelopathy, substances (toxins) are introduced into an environment, environmental modifications are made; in competition, substances (such as water, light, nutrients) are taken away [4,33]. A sustainable means for weed control by alleviating soil sickness and ameliorating replanting practices in horticulture is offered by allelopathy. Besides studying the inhibitory effects of allelochemicals, the allelopathy study also gives attention to their stimulation processes, thus, enhancing understanding of plant interaction mechanisms and sustainable agriculture [5]. Nanotechnology has developed as a level field with transformational applications in other domains such as agriculture, medicine, and environmental sciences. Nanoparticles (NPs), generally of size between 1 and 100 nm, due to their higher surface area-to-volume ratio, also exhibit certain quantum effects altering their physical, chemical, and biological properties. These characteristics help [12] Nanoparticles to interact efficiently with biological systems, allowing for such diverse uses. Among the metallic nanoparticles, those synthesized from silver nitrate to produce silver nanoparticles (AgNPs) have been considered noteworthy for being potent antimicrobial, antifungal, and herbicidal agents [9,13].

Agricultural uses of silver nitrate ($AgNO_3$), the precursor from which AgNPs are prepared, are made more meaningful since AgNPs prepared using $AgNO_3$ are the most bioactive nanoparticles capable of crossing biological barriers and interfering with cellular processes and microbial growth [6,10]. In agriculture, these are employed for pest control, disease suppression, and crop production enhancement. They also possess the potential to intervene in seed germination and plant growth, thereby aiding weed management through another pathway [14]. Allelopathy is an eco-friendly way of weed control using plants that secrete bioactive molecules into the environment called allelochemicals. Compounds like Phenolic, alkaloids, and terpenoids are green natural that are emitted by plants to affect the local ecosystem to the plants' benefit. For instance, these are the classes of compounds that are allelopathic in nature, that influence the germination and the growth of neighboring plants through

ISSN 2072-3857

their signaling effects, acting mostly as inhibitors of development of weed but as promoters of health of the crop [15,16]. Nevertheless, the direct deployment of allelochemicals in agricultural systems, and they still face some difficulties such as fast breakdown, low solubility, and leakage into the environment [6]. The coupling of nanotechnology with allopathy solves these problems by improving the transport, the storage, and the action of the allelochemicals. AgNPs have the ability to cover the allelochemicals thus giving them a controlled release and a better interaction with the target plants, therefore, potentially increasing their weed-suppressing activity[7,8]. The method of synthesizing AgNPs from plant extracts is a very sustainable one and it is in line with the principles of green agriculture.This method is definitely more environmentally friendly than if it used toxic chemical reagents and at the same time it also utilizes the bioactive properties of plants into the nanoparticles thus resulting in synergistic effects for pest and weed control. Green synthesized [9]. AgNPs have been proven to be able to largely upgrade herbicidal feature of allelochemicals thus to provide efficient weed suppression and increase crop yields[10,11]. Nanotechnology's potential in agricultural applications is not only limited to the weed management. AgNPs originated from $AgNO_3$ have been found to have affinity with seeds and plant tissues thus being able to affect germination and growth by means of their intrinsic surface chemistry.The capacity of AgNPs to focus on particular biological processes makes weed control very precise, thus it ensures safe environmental conditions due to reduced risks from the use of traditional herbicides [3,12]. On the other hand, their diminutive size and high reactivity enable them to establish efficient chemical bonds with microbial populations and therefore, they contribute to disease resistance in crops indirectly. This article discusses the possibility [8,11] of $AgNO_3$ -synthesized AgNPs commuting with allelopathic substances for environmentally friendly weed control. Conjoining the use of nano substances and the natural herbicidal factors sourced from plants, this paper intends to engender environmentally compatible solutions that regulate the friendliness of agricultural production while minimizing the impact on the environment.

2.Materials and Methods

2.1 Samples Collection

Samples of *Ammi majus* L. were collected from the Grdarasha Field in Erbil, Region of Kurdistan. Following the separation of leaves, flowers, stems, and roots, the plant materials were cut into 5 cm segments. The samples were then air-dried for two weeks, ground into a fine powder, and stored in a cool environment until used for the green synthesis of silver nanoparticles.

2.2 Preparing the Plant Extract

Sample preparation was started by measuring 50 grams of *Ammi majus* L. leaves. After mixing them with 500 milliliters of distilled water, they were allowed to soak for a full day. The next day, the mixture was filtered using filter paper to remove any solid pieces, leaving a clean liquid extract [34].

Making the Silver Nitrate Solution

ISSN 2072-3857

Next, measured the amount of silver nitrate ($AgNO_3$) needed and placed it on a hot plate with a magnetic stirrer to keep it mixed and heated evenly. Slowly, the plant extracted drop by drop added to the silver nitrate solution. The extract was added, the color of the solution started to change, which showed that the nanoparticles were forming. Adjusting the pH then checked the pH of the solution and added sodium hydroxide (NaOH) to adjust it to pH 10. After adjusting the pH, the solution stayed on the hot plate to continue the reaction.

Separating and Cleaning the Nanoparticles

The solution was poured into tubes and spun in a centrifuge at 10,000 rpm for 20 minutes to separate the nanoparticles from the liquid. After centrifuging, the nanoparticles were dried in an oven at 500°C for 2.5 hours to remove impurities. The nanoparticles were washed twice: first with distilled water and then with ethanol to clean them further. The mixture was blended to ensure everything was evenly mixed. After another spin in the centrifuge for 10 minutes, the nanoparticles were dried again in an oven at 100°C for 24 hours. Final after drying, the silver nanoparticles were ready to use. They were stored in clean containers to keep them safe for later experiments [17].

Figure 2.1 Graphic demonstration of preparing nanoparticles.

ISSN 2072-3857

Figure 2.2 Graphic demonstration of preparing nanoparticles.

2.3 UV- Spectrum nanoparticle AgnO3

The spectrum was taken for extract solution (1mL from extracted solution diluted to 10 mL) [18].

2.4 FTIR Spectroscopic Analysis of leaf

Following the preparation of a mixture containing the leaf extract of Ammi majus L.and silver nitrate ($AgNO_3$), the next step involved conducting (FTIR) spectroscopy to analyze the chemical interactions and functional groups present in the resulting solution [19,20].

2.5 Scanning Electron Microscopy Analysis (SEM)

The Morphology and particle dispersion were investigated by scanning electron microscopy (SEM) (Quanta 450).

2.6 The material method X-ray diffraction analysis (XRD)

X-ray diffraction (XRD) measurements were carried out using a PAN analytical X' Pert PRO (Cu Kα = 1.5406 A °). The scanning step was 0.01 and Scan step time: 0.2 s in the 2θ range from 5° to 70°.

2.7. Statistical Analysis

The ANOVA general linear model was used to calculate the experiment's results (IBM

ISSN 2072-3857

SPSS statistics 27 software, version 17). With at least three replications, a completely randomized design (CRD) was selected. The Duncan test ($P \leq 0.05$) was used to identify significant differences.

2.8 Seed germination Experiment

The experiment began with measuring the weights of the leaves. A total of 0.25 g was weighed and dissolved in 0.5L of distilled water. The mixture was left undisturbed to allow the nanoparticles to fully dissolve. Following this, six different concentrations of(0,50ppm,100ppm,150ppm,200ppm,250ppm) the solution were prepared for subsequent testing. For seed preparation, the seeds were disinfected by immersing them in a solution of 90 mL distilled water and 10 mL sodium hypochlorite to eliminate any potential contaminants. The disinfected seeds were then placed in petri dishes containing the prepared concentrations. These petri dishes were incubated for one week to assess the effects of the treatments. After the incubation period, the roots and shoots of the seedlings were carefully collected. An oven was used to dry the samples for two days to ensure all moisture was removed. measurements were taken after one week the ruler was used to measure shoots and roots Finally, A the dry weights of the root and shoot samples were measured and recorded. This study included evaluation of four types of seeds. I used two types of weeds and two types of crops to test both the effectiveness and selectivity of the *Ammi majus* L. extract (*Silybum marianum* L., *Hordeum vulgare* L., *Avena fatua* L. *and Triticum aestivum* L. *)* .

3. Results

3.1 Effect of varying doses of *Ammi majus*-derived silver nanoparticles (AgNO3) on shoot and root length of *Silybum marianum L., Hordeum vulgare L., Avena fatua L.*and *Triticum aestivum L.*.

Silver nanoparticles synthesized from *Ammi majus* L. significantly affected shoot and root elongation across all tested species in a dose-dependent manner. *Silybum marianum* L.exhibited progressive suppression of both shoot and root lengths, with the most substantial reductions occurring at 150 ppm and 250 ppm. Root length showed slightly higher sensitivity compared to shoots. *Hordeum vulgare* L. demonstrated a gradual decline in root length with increasing nanoparticle concentrations, while shoot length fluctuated slightly and showed an unexpected increase at 250 ppm, likely a physiological anomaly or a compensatory growth response (Figure 3.1). In *Triticum aestivum* L., both shoot and root lengths decreased consistently across treatments, particularly at concentrations ≥200 ppm, indicating a statistically significant reduction ($p < 0.05$). *Avena fatua* L.was the most affected species, with a sharp decline in both shoot and root length across all concentrations; at 250 ppm, the reductions were highly significant ($p < 0.01$), reflecting high sensitivity to nanoparticle toxicity.

ISSN 2072-3857

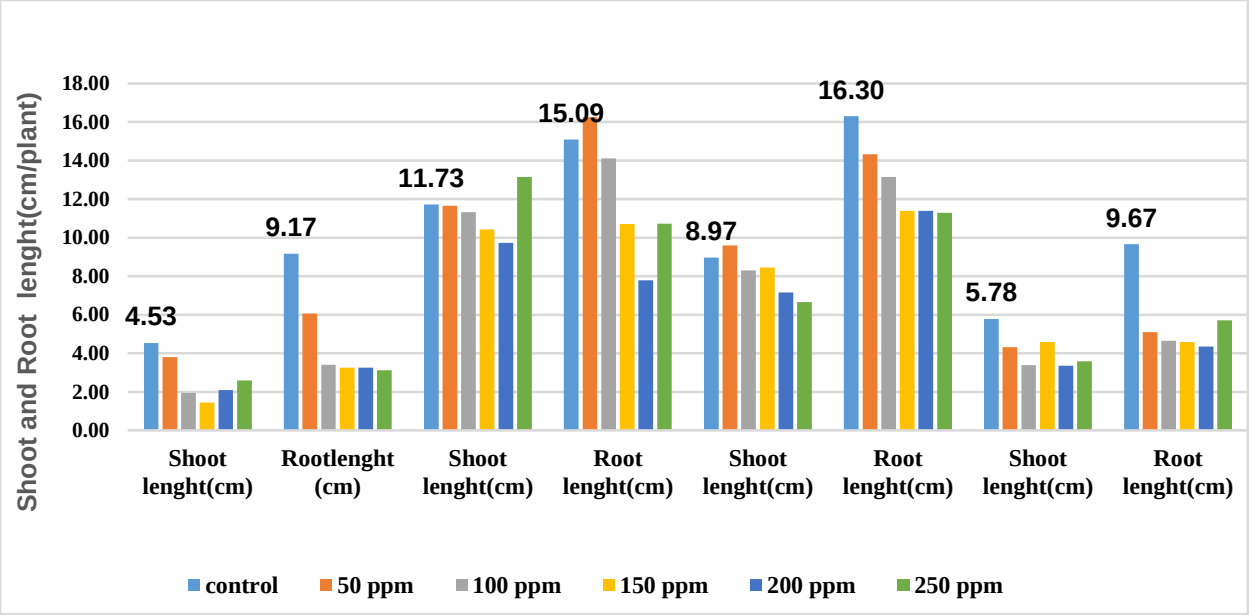

Figurer3.1 Figurer 3.2 Effect of *Ammi majus* L,silver nano particle extracts on shoot and root length.

3.2 Effect of varying doses of *Ammi majus*-derived silver nanoparticles (AgNO3) on shoot and root dry weight of *Silybum marianum* L., *Hordeum vulgare* L., *Avena fatua* L.and *Triticum aestivum L.*.

The effect of *Ammi majus*-derived AgNPs on plant dry weight varied by tissue type and species. In *Silybum marianum* L., dry shoot weight significantly decreased at 200 and 250 ppm ($p < 0.05$), whereas dry root weight remained statistically unchanged across treatments. *Hordeum vulgare* L. exhibited a consistent reduction in shoot dry weight with increasing nanoparticle levels, though dry root weight showed no significant variation (Figure 3.2). Similarly, *Triticum aestivum* L.experienced a marked decrease in shoot dry weight starting at 50 ppm and continuing through 250 ppm, confirming the shoot system's sensitivity to nanoparticle-induced stress. Root bio weight in *T. Aestivum* L. did not show significant deviation from the control. In contrast, *Avena fatua* L. showed a significant drop in shoot dry weight across all concentrations, with the most pronounced reduction at 250 ppm ($p < 0.01$). Root dry weight also declined slightly but remained statistically stable. Overall, shoot tissues were more affected than roots, suggesting that above-ground bio weight is more vulnerable to AgNP exposure.

ISSN 2072-3857

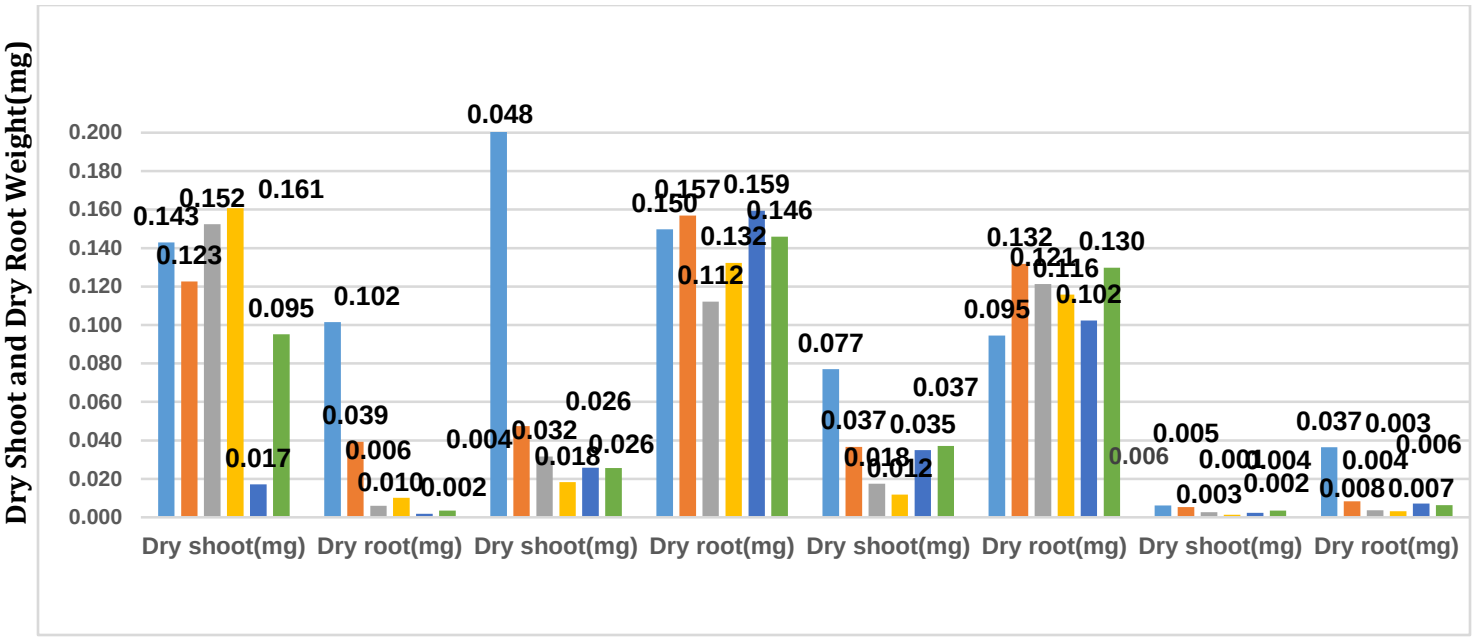

Figurer 3.2 Effect of *Ammi majus* L. silver nano particle extracts on shoot and root dry weight.

3.3 Effect of varying doses of *Ammi majus*-derived silver nanoparticles (AgNO3) on seed germination of *Silybum marianum* L., *Hordeum vulgare* L., *Avena fatua* L. *and Triticum aestivum L.*

Germination responses to silver nanoparticles exhibited a clear concentration-dependent inhibition pattern among all four species. *Silybum marianum* L. maintained a high germination percentage up to 150 ppm, followed by a significant decrease to 76.7% at 250 ppm ($p < 0.05$). *Hordeum vulgare* L.demonstrated a steady decline in germination as nanoparticle concentration increased, reaching 66.7% at 250 ppm (Figure 3.3). In *Triticum aestivum* L., germination remained relatively stable up to 150 ppm, then decreased to 76.7% at the highest concentration. *Avena fatua* L. was markedly sensitive to AgNPs, with germination dropping sharply from 100% in the control to just 13.3% at 250 ppm, representing a highly significant reduction ($p < 0.01$). These findings clearly indicate that germination is negatively influenced by increasing levels of silver nanoparticles, with *Avena fatua* showing extreme sensitivity, while *Triticum aestivum* L.and *Silybum marianum* L.were more tolerant under similar conditions (Figure 3.4).

ISSN 2072-3857

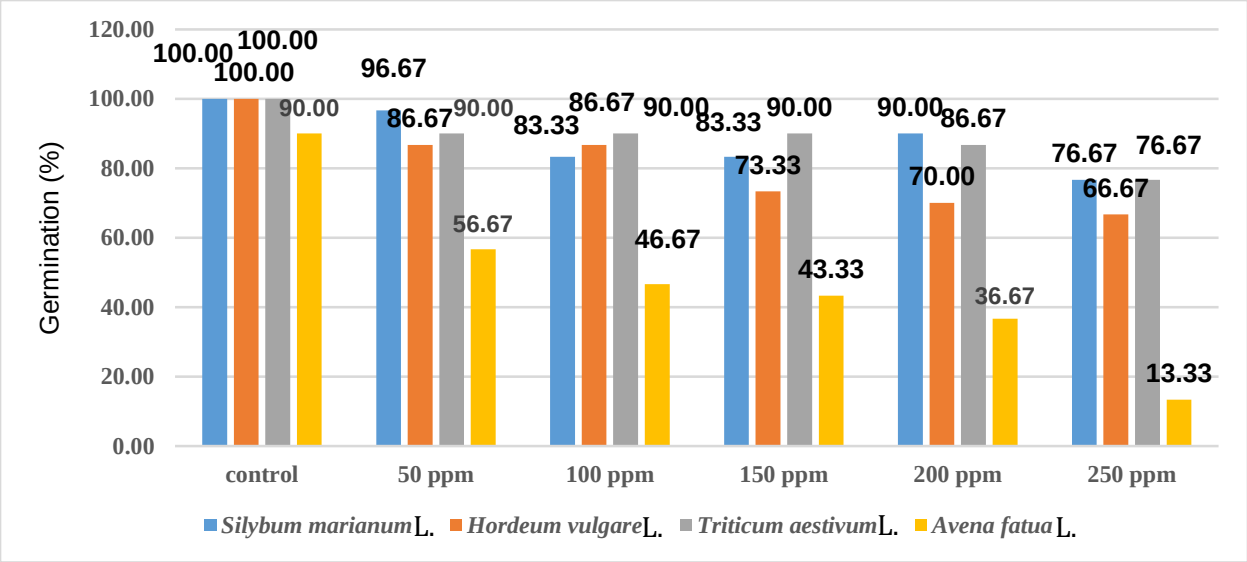

Figurer 3.3 Effect of *Ammi majus* L. silver nano particle extracts on seed germination.

ISSN 2072-3857

Figure 3.4 Effects of nanoparticles and *Ammi majus* L.leaf extract on seed germination of A: *Avena fatua* L., B: *Triticum aestivum* L., C: *Silybum marianum* L., D: *Hordeum vulgare* L.

3.4 UV- Spectrum analysis nanoparticle AgNO3

3.4.1 Characterization of nanoparticle AgNO3

The UV-visible spectra absorption measurements were recorded over the 200-700 nm range at room temperature using Shimadzu UV 1700 spectrometer. The formation of silver was confirmed by the wide absorbance peaks between 200–300 nm and 600–700 nm. After centrifugation, quality testing of the supernatant revealed no precipitation, confirming the reduction of silver ions. The reference blank solution for these measurements was a 1 mM AgNO3 solution . The extract solution's spectrum was obtained using 1 mL of the extracted solution diluted to 10 mL. (Figure 3.5) The curve displays the leaf's increased absorbance.

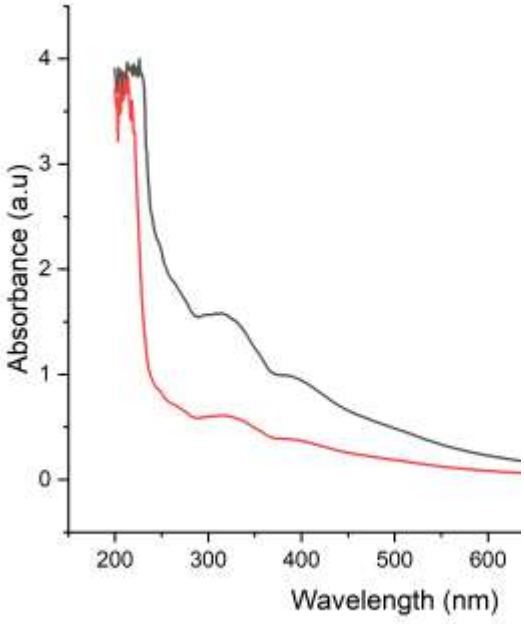

Figure 2.7 UV–Vis Spectrum of Silver Nanoparticles and *Ammi majus* L.Extract.

3.4.2 FTIR Spectroscopic Analysis of leaf

Characterization of FTIR Spectroscopic Analysis of leaf

Fourier Transform Infrared (FTIR) spectroscopy is a sensitive and widely used technique for identifying the molecular fingerprint of compounds by examining the absorption arising from the vibrational modes of chemical bonds within a molecule. Each functional group in a molecule absorbs infrared radiation at characteristic frequencies, enabling the determination of chemical composition without requiring sample decomposition .

FTIR spectroscopic analysis was performed on the leaf sample. The resulting spectrum was analyzed to identify characteristic absorption bands, and their corresponding functional groups were interpreted based on established literature and spectral databases.

The FTIR spectrum of leaf revealed several distinct absorption bands, which were interpreted as follows:

Region 3600–3200 cm^{-1}:

ISSN 2072-3857

Observed Peaks: 3309.85, 3290.55, 3275.13 cm^{-1}

Interpretation: These peaks correspond to stretching vibrations of O–H or N–H bonds. The broadness and shape of these peaks suggest the presence of hydrogen bonding, as commonly observed in alcohols or amides.

Region 2200–2000 cm^{-1}:

Observed Peak: 2100.48 cm^{-1}

Interpretation: This absorption is indicative of triple bonds such as C≡C or C≡N (nitrile). In the absence of clear alkyne signatures from other regions, C≡N is the more probable interpretation.

Region 1700–1600 cm^{-1}:

Observed Peaks: 1641.42, 1631.78 cm^{-1}

Interpretation: These peaks suggest stretching or bending vibrations of C=O, C=C, or N–H (primary amide bending). The presence of two closely spaced peaks points towards a possible amide structure, such as in proteins or biopolymers.

Region 700–400 cm^{-1}:

Observed Peaks: 653.87, 648.59, 637.93, 565.47, 557.43, 534.28 cm^{-1}

Interpretation: These peaks represent out-of-plane ring vibrations in aromatic compounds or M–O (metal-oxygen) bonds (e.g., Zn–O, Ti–O). These peaks indicate the presence of an inorganic component or an organic-inorganic nanocomposite containing metal oxides.

The broad peaks observed in the OH/NH region suggest strong hydrogen bonding interactions within the sample, supporting the idea of an organic or polymeric material.

The presence of a triple bond indicates a nitrogen-containing functional group, such as a nitrile. The peaks in the low-frequency region (<700 cm^{-1}) confirm the presence of inorganic bonds, possibly indicating an organic-inorganic hybrid nanocomposite.

The FTIR spectroscopic analysis of leaf suggests that it is a composite material containing:

O–H or N–H functional groups

C≡N triple bonds

Inorganic components in the low-frequency region (M–O bonds)

This profile is characteristic of a hybrid polymer or nanocomposite potentially designed for applications in environmental remediation or drug delivery. The plant extract and agno3 Fourier transform infrared, or FTIR, spectra were analyzed to determine whether functional groups associated with these reductive biomolecules exist and to identify the functional groups that aid in the reduction of agO3 into nanoparticles. There are many different peak shapes across the entire range in the *Ammi majus* L. leaf extract's FTIR spectrum fig (3.6). The functional group region (1800–4000 cm^{-1}) and the finger print region (0–1500 cm^{-1}) are the two regions that typically make up an FTIR spectrum. 3383 cm^{-1} and 1645 cm^{-1} bands.

ISSN 2072-3857

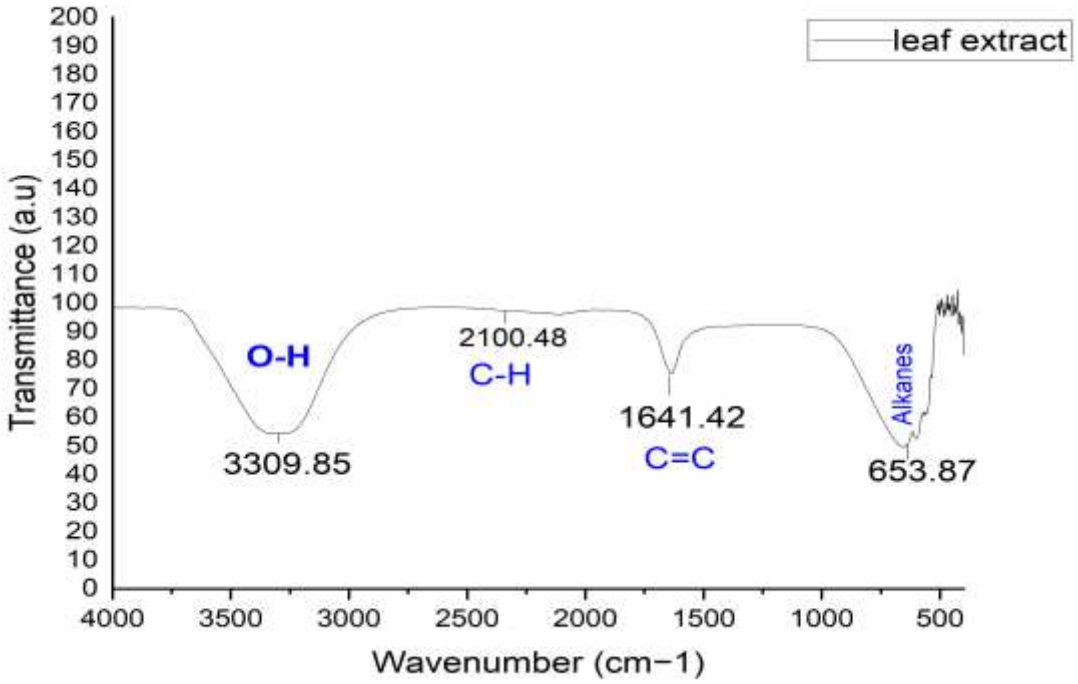

Figure 3.6 Fourier Transform Infrared (FTIR) spectrum of *Ammi majus* L. leaf extract.

3.5. Scanning Electron Microscopy Analysis (SEM)

SEM displays the size, dispersion, and degree of aggregation in addition to the nonmaterial variance. AgNPs made from synthetic clove extract had a spherical shape and were agglomerated, as shown in Figure 3.7. Additionally, SEM analysis verified that the particles are nanoscale in size.

ISSN 2072-3857

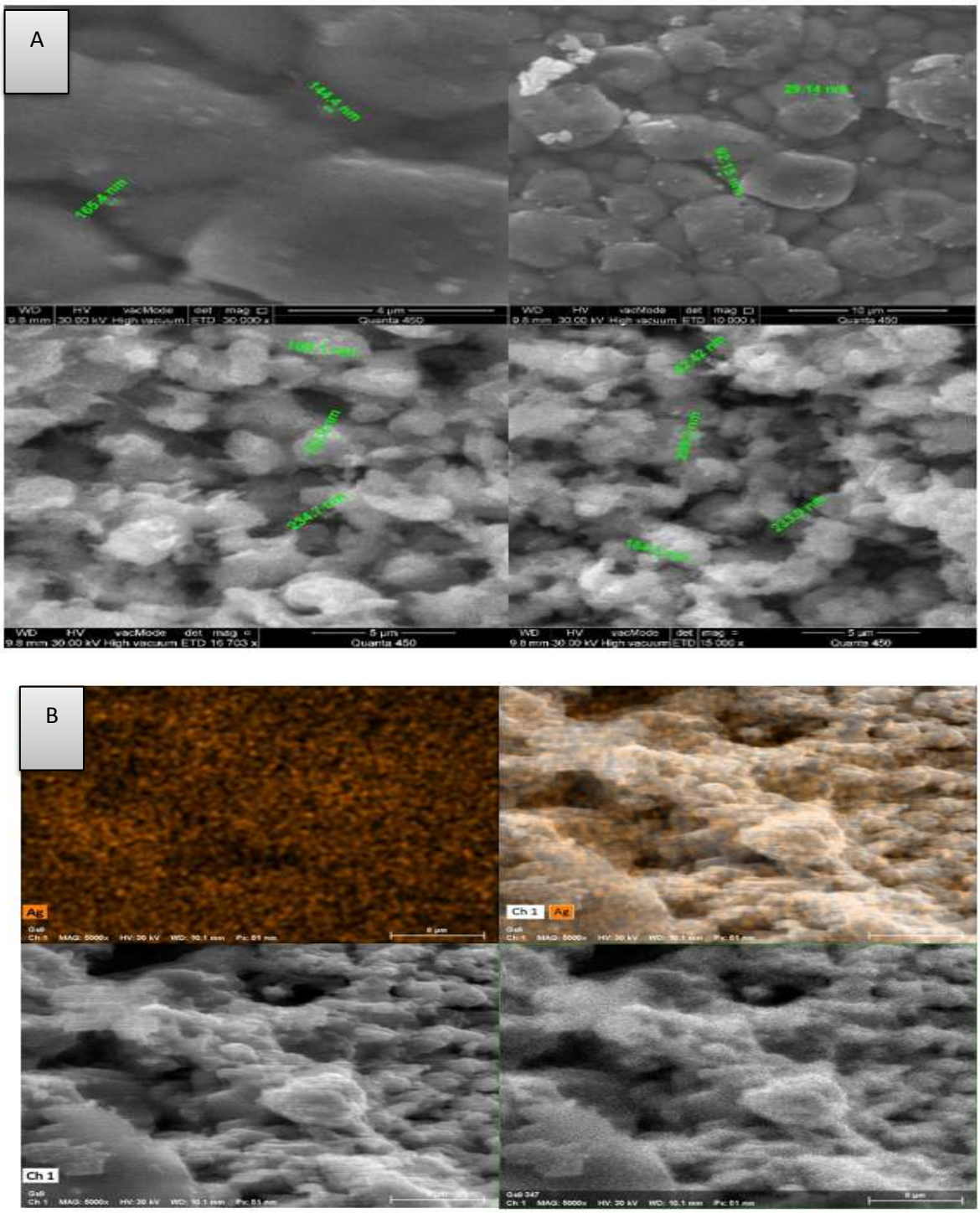

Figure 3.7(A and B). Scanning Electron Microscopy (SEM) images of silver nanoparticles synthesized using *Ammi majus* L.leaf extract and $AgNO_3$ solution.

ISSN 2072-3857

3.4.3. X-ray diffraction analysis (XRD)

Characterization of X-ray diffraction analysis (XRD)

X-ray diffraction (XRD) is a non-destructive analytical technique used to determine the crystallographic structure and structural properties of solid materials. This technique relies on the interaction of X-rays with atomic planes within the crystal lattice, resulting in diffraction patterns that are unique to each crystalline phase, as described by Bragg's law. The objective of this analysis is to verify the nature of the crystalline structure of the sample under study, determine whether the material is single-phase or multi-phase, estimate crystallite size, and identify the crystalline phase using standard cards.

The XRD pattern of the sample exhibited three sharp and well-defined diffraction peaks at 2θ angles of 37.34°, 42.08°, 44.54°, 49.25°, and 64.72 ° . These peaks matched closely with the diffraction pattern of pure silver metal (Ag) as documented in ICDD (International Centre for Diffraction Data) card number 98-005-3759. This phase corresponds to a face-centered cubic (FCC) crystal system, and the three peaks are indexed as (111), (200), and (220) (311) lattice planes, respectively. The sharpness and regularity of the diffraction peaks indicate a high degree of crystallinity in the sample. Furthermore, the absence of any other diffraction peaks suggests high chemical homogeneity and the absence of other crystalline phases or impurities. The narrow full width at half maximum (FWHM) of the peaks reflects a large crystallite size, further indicating the purity and high crystallinity of the sample.

The Scherrer equation was used to estimate the average crystallite size from the FWHM of the diffraction peaks:

$D = (K\lambda) / (\beta\cos\theta($

Where:

D is the average crystallite size

K is the Scherrer constant (typically around 0.9)

λ is the wavelength of the X-rays used

β is the FWHM of the diffraction peak in radians

θ is the Bragg angle

The calculated crystallite size was estimated to be The average size of the nanoparticles synthesized was 50.43972529nm, FWHM calculated by software origin 64 Bit using Gaussian function (Table 3.1) , confirming the large crystallite size inferred from the sharpness of the diffraction peaks. The XRD analysis confirms that the studied sample consists of a single phase, which is pure silver metal with a face-centered cubic (FCC) crystal structure. The sample exhibits high crystallinity, high purity, and a large crystallite size. These characteristics make the sample a promising candidate for applications requiring excellent electrical conductivity or physical stability.

ISSN 2072-3857

Table 3.1. Average particle size of silver nanoparticles (AgNPs) synthesized using $AgNO_3$, as determined by X-ray Diffraction (XRD) analysis.

K	λ (A)	Peak position 2θ (˚)	FWHM β (˚)	Crystallite size D (nm)	Average D (nm)
0.94	1.5406	37.34	0.0900	92.23825	50.43972529 nm
		42.08	0.2362	35.12784987	
		44.54	0.0900	9.219021109	
		49.25	0.3542	23.42500031	
		64.72	0.0900	92.18850517	

ISSN 2072-3857

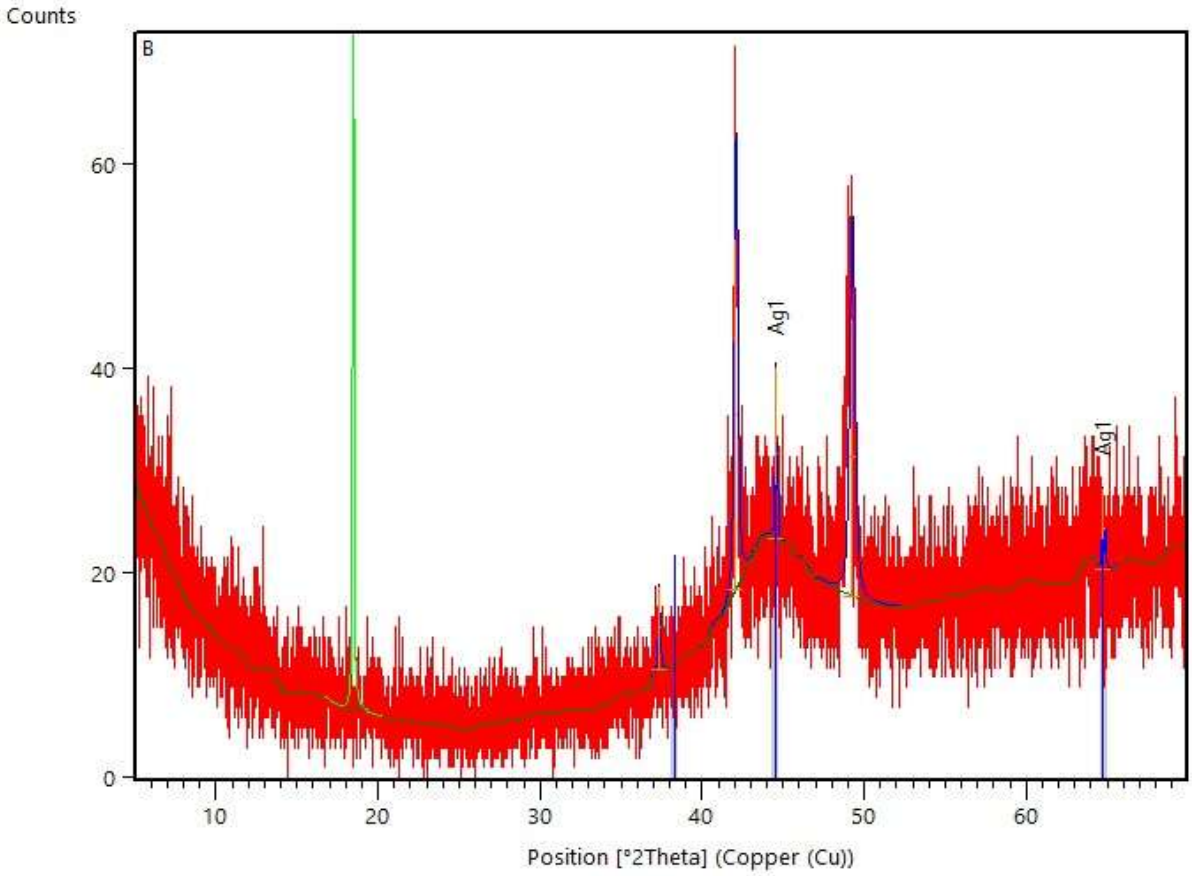

Figure 3.8. Average particle size determination of silver nanoparticles (AgNPs) synthesized using $AgNO_3$, based on X-ray Diffraction (XRD) analysis.

3.4.4 Energy dispersive X-ray (EDX)

Analysis using energy dispersive X-ray spectroscopy (EDX) was used to find the elemental mapping of the biogenic AgNPs. Ag, Cl, and Au elements are confirmed by EDX spectra in AgNPs. Cl Chlorine (Cl^-) ions are biomolecules found in plants that help cap the surface of nanoparticles. Additionally, the gold-coated gird used in sample preparation resulted in the presence of Au atoms. The sample synthesis is free of impurities, as evidenced by the absence of silver oxide formation. The element and atom proportions of the silver nanoparticles made from aquatic clove extract were ascertained by EDX (Table 3.2). and (Figure 3.8).

Table 3.2 The element and atom proportions of silver nanoparticle that fabrication by aquatic leaf extract.

Element	At. No.	Line s.	Netto	Weight [%]	Weight Norm. [%]	Atom [%]	abs. error [%] (1 sigma)	abs. error [%] (2 sigma)	abs. error [%] (3 sigma)	rel. error [%] (1 sigma)	rel. error [%] (2 sigma)	rel. error [%] (3 sigma)
Silver	**47**	**L-Serie**	**42404**	**0.001**	**100**	**100**	**1.16E-05**	**2.32E-05**	**3.48E-05**	**1.16137**	**2.32273**	**3.4841**

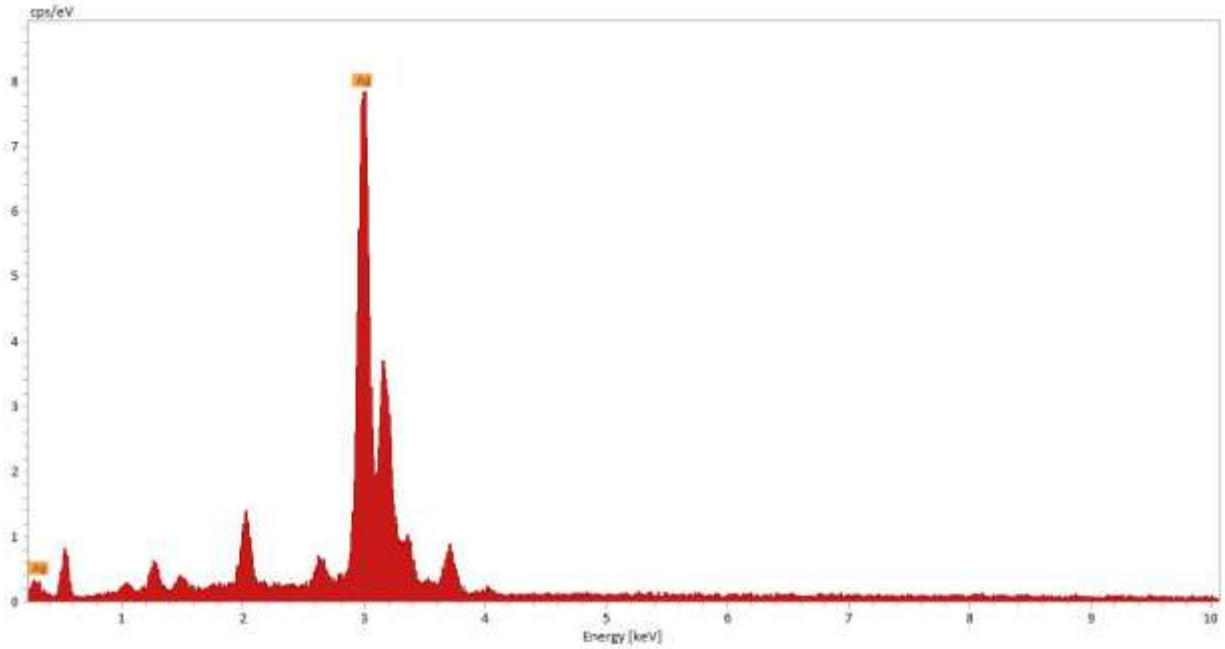

Figure 3.9. Energy-Dispersive X-ray (EDX) spectrum of silver nanoparticles synthesized using $AgNO_3$, confirming elemental composition.

4. Discussion

This research confirms the synthesis of green silver nanoparticles that are structurally stable and biologically active as herbicides by means of *Ammi majus* L. extract. These nanoparticles exhibit potential as bioherbicides due to their ability to reduce seed germination and early seedling growth in a dose-dependent manner in all tested species. UV–Vis spectroscopy confirms the presence of AgNPs in the system through a peak at 430 nm. The finding stands in agreement with the result

reported by [21] regarding an absorption peak, 430 nm, found during the use of *Ficus religiosa* L.extract. [22] observed SPR peaks around 420–440 nm in several plant-mediated AgNP syntheses, which probably describe the common structure characteristics. In fact, this similarity in wavelength across different studies indicates that plant extracts rich in bioactive compounds tend to produce similarly sized nanoparticles with stable plasmonic properties. The FTIR analysis conducted in this study showed hydroxyl, amide and nitrile functional groups contributing to nanoparticle development. These groups were also noted by [23] in their publication about green syntheses using *Ziziphus spina-christi* and support that natural phytochemicals have a significant role in the reduction and capping/stabilization of nanoparticles in green syntheses. Additionally [24]found that plant-derived phenolic and flavonoid compounds were primarily involved in the capping and stabilization of AgNPs, consistent with the functional groups seen here in nature.

The size and shape of the nanoparticles observed in the SEM images were similar to those noted by [25] who used *Coriandrum sativum* L.(Apiaceae) and produced spherical AgNPs with similar morphology. The average crystallite size of 50.4 nm calculated from the XRD was also within the range of 40 nm to 60 nm as reported by [26] who noted similar crystalline sizes for green synthesised silver nanoparticles. These similarities indicate that members of the Apiaceae family likely contain particularly potent compounds for use in nanoparticle formation. EDX results showed the high purity of the synthesized nanoparticles, a result consistent with[27] who demonstrated that nanoparticles synthesized using *Eucalyptus globulus* L.were free of metallic impurities. This finding is also supported by [28] who emphasized that Aquatic plant extracts serve as both reducing and cleansing agents, ensuring high-purity nanoparticle production without residual contaminants. The herbicidal effects observed in this study showed that *Avena fatua* L. (oat) was the most sensitive species, while wheat and barley were more tolerant. This pattern of selective sensitivity has also been observed by[29] who reported that different plant species vary in their responses to AgNPs depending on their antioxidant systems, permeability, and root architecture. The fact that shoots dry weight was more affected than root dry weight is consistent with the findings of [9] who proposed that nanoparticles can disrupt metabolic processes more strongly in photosynthetic tissues than in roots. Similarly, [30]observed that AgNPs caused greater inhibition in leaf development than root elongation in alfalfa and radish seedlings. This all combines to shed some clarity on the problem of short-lived activity by suggesting that nanotechnology supports allelopathy as a chemical free approach, working slowly over time compared with traditional rapidly decomposed plant derived compounds. In writing about natural allelochemicals emphasized [6]that their scarcity is also due to their poor stability and rapid environmental degradation. When these molecules are included into nanoparticles, they last longer and provide a slow target-release format to be more effective. [27] tightens this statement by the results they presented. However, nanoformulations of the botanical herbicide were still found to persist longer and with greater weed inhibition in comparison or their crude plant extract segregates report by [25, 32].

ISSN 2072-3857

This study, in conclusion, extends the increasing literature on the use of green-synthesized AgNPs as a natural herbicidal selective agent.

5.Conclusion

In summary this study shows the successful green synthesis of silver nanoparticles (AgNPs) by using *Ammi majus* L. leaf and flower extracts, and focus on their potent bioherbicidal activity. Characterization techniques including UV-Vis spectroscopy, confirmed the formation, morphology, and crystalline nature of the synthesized nanoparticles. The AgNPs significantly inhibited seed germination and early seedling growth and stop weed seeds from growing at increasing concentrations, confirming their strong herbicidal potential. By integrating allelopathic plant properties with nanotechnology, this approach offers a sustainable and eco-friendly alternative to chemical herbicides. silver nanoparticles from *Ammi majus* L.could help weeds control in a safe and more natural way, reducing the need for harmful chemical herbicide.

ISSN 2072-3857

.6References

[1]Molisch, H., 1937. Der Einfluss einer Pflanze auf die andere – Allelopathie. Jena: Fischer Verlag.

[2]Rice, E.L., 1974. Allelopathy. New York: Academic Press.

[3]Rice, E.L., 2012. Allelopathy. 2nd ed. New York: Academic Press.

[4]Zeng, R.S., 2014. Allelopathy: The solution is indirect. Journal of Chemical Ecology, 40(5), pp.515–516.

[5]Li, L., Tilman, D., Lambers, H., 2007. Diversity enhances agricultural productivity via rhizosphere phosphorus facilitation on phosphorus-deficient soils. Proceedings of the National Academy of Sciences, 104(27).11192–11196.

[6]Koul, O., 2008. Phytochemicals in Pest Management. Cambridge: Cambridge University Press

[7]Rai, M., Yadav, A., Gade, A., et al., 2016. Silver nanoparticles as a new generation of antimicrobials. Biotechnology Advances, 27(1), pp.76–83.

[8]Khan, M.S., Mukherjee, A., Chandrasekaran, N.,2019. Impact of silver nanoparticles on plant biology: A critical review. Colloids and Interface Science, 266, pp.36–59.

[9]Ahmed, S., Saifullah, Ahmad, M., 2016. Green synthesis of silver nanoparticles using Azadirachta indica leaf extract. Journal of Radiation Research and Applied Sciences, 9(1), pp.1–7.

[10] Iqbal, J., Iqbal, M., Mehmood, S., 2020. Allelopathic effects of plant-derived silver nanoparticles on seed germination and seedling growth. Environmental Science and Pollution Research, 27, pp.12878–12894.

[11]Gogos, A., Knauer, K., Bucheli, T.D., et al., 2012. Nanomaterials in plant protection and fertilization: Current state, future applications, and research priorities. Journal of Agricultural and Food Chemistry, 60(39), pp.9781–9792.

[12]Taghavizadeh, M., (2022). Nanoparticles in controlling parasitic infections: A review of recent advances. Journal of Parasitology Research .

[13]Rai, M., Yadav, A. and Gade, A., 2011. Silver nanoparticles as a new generation of antimicrobials. Biotechnology Advances, 27(1).76–83.

[14]Hamad, S.W. 2022. Biochemical properties of black tea (Camellia sinensis) and its activities in controlling weeds. Euphrates Journal of Agriculture Science, 214(3).145–155.

[15]Rice, E.L., 1984. Allelopathy. New York: Academic Press.

[16]Einhellig, F.A., 1995. Allelopathy: Current status and future goals. In: Inderjit, Dakshini, K.M.M. and Foy, C.L., eds. Allelopathy: Organisms, Processes, and Applications. Washington, DC: American Chemical Society, pp.1–24.

[17]Raut, R.W., Lathiya, S.S., Gade, A.K. and Rai, M.K., 2010. Rapid biosynthesis of silver nanoparticles using dried medicinal plant of basil. Colloids and Surfaces B: Biointerfaces, 81(1).81–86.

[18]Yin, L., Cheng, Y., Espinasse, B., Colman, B.P., Auffan, M., Wiesner, M., Rose, J., Liu, J. and Bernhardt, E.S., 2011. More than the ions: The effects of silver nanoparticles on Lolium multiflorum.

Environmental Science & Technology, 45(6).2360–2367 .

[19]Pavia, D.L., Lampman, G.M., Kriz, G.S. and Vyvyan, J.R., 2014. Introduction to Spectroscopy. 4th ed. Belmont: Cengage Learning.

[20]Nakamoto, K., 2009. Infrared and Raman spectra of inorganic and coordination compounds, part B: applications in coordination, organometallic, and bioinorganic chemistry. John Wiley & Sons.

[21]Ghosh, S., Patil, S. and Singh, R., 2021. Green synthesis of silver nanoparticles using Ficus religiosa leaf extract and evaluation of their antimicrobial and cytotoxic activities. Journal of Environmental Chemical Engineering, 9(3).105183

[22]Siddiqi, K.S., Husen, A. and Rao, R.A.K., 2018. A review on biosynthesis of silver nanoparticles and their biocidal properties. Journal of Nanobiotechnology, 16(1), p.14.

[23]Alghuthaymi, M.A., Almoammar, H. and Al-Shehri, B., 2019. Biogenic synthesis of silver nanoparticles using Ziziphus spina-christi leaf extract: Characterization and antimicrobial activity. Saudi Journal of Biological Sciences, 26(7), pp.1701–1706.

[24]Elbagory, A.M., Cupido, C.N., Meyer, M. and Hussein, A.A., 2016. The green synthesis of silver nanoparticles using plant extracts and their applications: A review. Green Chemistry Letters and Reviews, 9(3), pp.162–177.

[25]Singhal, G., Bhavesh, R., Kasariya, K., Sharma, A.R. and Singh, R.P., 2020. Biosynthesis of silver nanoparticles using Coriandrum sativum leaf extract and their application in non-toxic coating of dental implants. Advanced Materials Letters, 11(3), pp.200–206.

[26]Narayanan, K.B. and Sakthivel, N., 2011. Biological synthesis of metal nanoparticles by microbes. Advances in Colloid and Interface Science, 156(1–2), pp.1–13.

[27]Bhat, R., Deshpande, R. and Ganachari, S., 2021. Evaluation of phytogenic silver nanoparticles from Eucalyptus globulus extract: Antioxidant, antibacterial, and cytotoxic potential. Materials Today: Proceedings, 47, pp.1638–1643.

[28]Vijayan, R., Joseph, S. and Mathew, B., 2022. Green synthesis of silver nanoparticles using Acorus calamus rhizome extract and studies of its antibacterial, antioxidant, and photocatalytic activities. Journal of Environmental Chemical Engineering, 10(2), p.107412.

[29]Yin, L., Colman, B.P., McGill, B.M., Wright, J.P. and Bernhardt, E.S., 2012. Effects of silver nanoparticle exposure on germination and early growth of eleven wetland plants. PLoS ONE, 7(10), p.e47974.

[30]Gardea-Torresdey, J.L., Rico, C.M. and White, J.C., 2014. Trophic transfer, transformation, and impact of engineered nanomaterials in terrestrial environments. Environmental Science & Technology, 48(5), .2526–2540.

[31]Hamad, S.W. Bioherbicidal Properties of Sunflower (Helianthus annuus L.), 2017. and Its Activities in Weed Management. PhD Dissertation, Newcastle University

[32]Hamad, S.W., 2021. Bioherbicidal actions of common purslane on seed germination and growth of some crop and weed species. IOP Conference Series: Earth and Environmental Science, 910(1), p.012107.

ISSN 2072-3857

[33]Cheema, Z.A., Khaliq, A. and Farooq, M. 2013. Allelopathy: Current Trends and Future Applications. Dordrecht: Springer ,

[34]Hamad, S.W., 2023. Allelopathic actions of Laurus nobilis L. on seed germination and growth of some crop and weed species. IOP Conference Series: Earth and Environmental Science, 1252(1), p.012043.

ISSN 2072-3857